Analytical Model of Permanent Magnet Synchronous Machine in/around Resonance

D. Pejovski, A. Di Gerlando, G. M. Foglia, R. Perini

***Abstract* -- In this paper an analytical model of a permanent magnet synchronous motor (PMSM) drive in/around torsional resonance is developed in the dq frame. The model accounts for electrical and mechanical aspects of the system, emphasizing their coupling and effects regarding voltage, torque and speed harmonics. Its aim is to obtain simple formulae which can predict electromagnetic and shaft torque response to a harmonic voltage supply, often present in variable speed drives. The model is solved by applying the small variations method and transfer functions formalism. The solution allows for predicting system behaviour in different operating conditions, especially important in/around resonance. The results are verified by extensive simulations in Matlab/Simulink environment.**

***Index Terms*--Torsional vibrations, shaft torque, harmonic voltage**

I. Introduction

In variable-speed drives including a power converter, almost any kind of modulation technique produces voltage harmonics which are injected in the system besides the fundamental component. This is due to the discrete switching of the power semiconductors and the generated harmonics are related to the drive topology, switching frequency, motor parameters, control algorithm, etc. [1]. These voltage harmonics give rise to line current harmonics, which, in turn, result in electromagnetic torque harmonics. Consequently, shaft oscillations occur which are reflected in the measurements and affect the control system as well.

Many researchers have been dealing with torsional analysis, investigating the causes for torsional vibrations and, more importantly, various damping methods. In [2], an extensive mathematical analysis of pulsating torque components in ac machines is presented. The paper provides tools for predicting their locations in the frequency domain, as well as their amplitudes. However, the developments are not accurate for low-power machines in low-speed regions away from their rated operating points. Moreover, in the computations current amplitudes are used without clarifying how they can be obtained. In [3], the authors state out that, after identifying the voltage harmonics, the current harmonics can be found in a straightforward way from the motor steady-state stator impedance.

In [4], a torque harmonic with magnitude 0.02p.u. at frequency equal to the system natural frequency excites the resonance. Simulations through equivalent electrical circuits are presented to confirm that torque harmonic frequency is much more important than its amplitude. However, only the mechanical system is analysed, without considering the interaction with its electrical companion and the conclusions are not experimentally confirmed.

The authors in [5] present a methodology for torque harmonic prediction excited by a speed harmonic in induction motors (IMs). Although the analysis outcome has been confirmed in practice, it is not clear how it can be extended to PMSM, the procedure is iterative and does not account for the coupling characteristics.

In a few papers, like [6] and [7], the electromagnetic phenomena are represented in the torsional vibration analysis by an equivalent stiffness and damping. Consequently, the natural frequencies increase even up to 8-10 percent, particularly evident in case of "soft" couplings. However, [6] regards only IMs at constant speed, while [7] deals with reciprocating machinery where torque oscillations occur at multiples of the running speed. Both publications do not provide mathematical tools for predicting the expected torque harmonics amplitudes.

Some researchers, on the other hand, consider that electrical and mechanical systems do not affect each other due to the large difference between their time constants, thus electrical and mechanical dynamics can be analysed separately [8]. This is true only in certain applications, like wind energy conversion systems, but not for servomotor drives.

In this paper, a theoretical model of the electromechanical interactions in a PMSM coupled with its load is presented in Section II, considering both the PMSM dq-frame model and the mechanical two-degree-of-freedom model. Above all, the behaviour close to resonance is pointed out. The dynamical electrical equations are extended to include a harmonic in the supply voltage. Furthermore, differential equations describing the mechanical aspects are added and the small variations method is applied to the overall system. After solving it in the Laplace domain, relationships between harmonic excitations and system response are obtained. Moreover, straightforward formulae for predicting electromagnetic and shaft torque harmonic amplitudes are derived. In Section III, the theoretical results are verified in Matlab/Simulink at various operating points, i.e. in a wide range of excitation frequencies, particularly important about/in resonance conditions. Conclusions are presented in Section IV. This analytical model could be a particularly useful tool for identifying critical points when a rotating system approaches resonance and for providing knowledge of potentially dangerous torques that can be generated.

Authors are with the Department of Energy at Politecnico di Milano, Via La Masa 34, 20156 Milano, Italy.

e-mails: dejan.pejovski@polimi.it, antonino.digerlando@polimi.it, gianmaria.foglia@polimi.it, roberto.perini@polimi.it.

II. Analytical Model

The objective of this analysis is to create a simplified analytical model which can predict the electromagnetic and the shaft torque harmonics excited by a PWM voltage harmonic component, particularly close to resonance. The model includes both electrical and mechanical system aspects, i.e. the dynamical equations of a synchronous PMSM in the dq-frame, differential equations for a 2 degree-of-freedom (DOF) system and a load angle equation. A simplified representation of the analysed system is shown in Fig. 1, while the block-diagram of the input-output effects chain is shown in Fig. 2.

A typical control for this kind of systems is realised in the dq-frame and consists of internal current loop and external speed loop. The lower the cutoff frequency of the current loop, the more the system becomes voltage driven.

A. Electrical Aspects of the System

The electromagnetic fluxes of a PMSM in the dq-frame can be expressed in the time domain as:

$$\begin{cases} \Psi_d = L_d i_d + \Psi_{PM} \\ \Psi_q = L_q i_q \end{cases} \tag{1}$$

where L_d=L_q=L is the synchronous inductance of an isotropic motor, Ψ_{PM} is the permanent magnet flux and i_d and i_q are the dq current components.

The well-known stator voltage equations are:

$$\begin{cases} v_d = Ri_d + p\Psi_d - \dot{\theta}\Psi_q \\ v_q = Ri_q + p\Psi_q + \dot{\theta}\Psi_d \end{cases} \tag{2}$$

where R is the motor phase resistance, $\dot{\theta}$ is the motor electrical angular speed and p stands for time derivative.

Let us assume that the motor supply voltage consists of a fundamental v_1 and only one harmonic component v_h resulting from the switch-mode inverter sinusoidal PWM modulation:

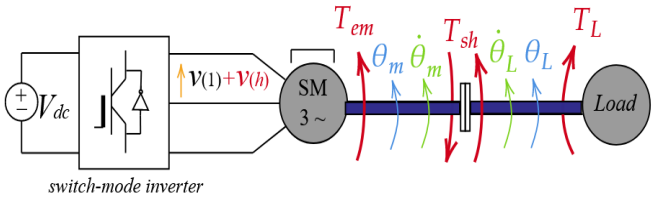

Fig. 1. System under study consisting of a power supply, switch-mode inverter, a 3-phase PMSM and a load.

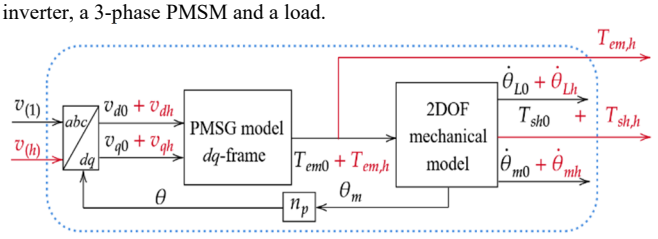

Fig. 2. Block-diagram of the developed analytical model. In red are the variables subject to analysis. Subscripts 0 and *h* stand for steady-state value and harmonic oscillation, respectively.

$$\begin{cases} v_a = v_{a1} + \sqrt{2}V_h \cos[h_v\omega_1 t] \\ v_b = v_{b1} + \sqrt{2}V_h \cos\left[h_v\left(\omega_1 t - \frac{2\pi}{3}\right)\right] \\ v_c = v_{c1} + \sqrt{2}V_h \cos\left[h_v\left(\omega_1 t + \frac{2\pi}{3}\right)\right] \end{cases} \tag{3}$$

where V_h is the harmonic magnitude rms value, h_v is the voltage harmonic order and ω_1 is the fundamental angular frequency.

Equation (3) can be represented in the dq-frame by applying the Park transform $T(\theta)$ on v_1 and v_h separately and superposing the outcomes. In case of positive/negative sequence harmonics, we get respectively:

$$\begin{cases} v_d = \sqrt{3}V_1 \sin\delta - \sqrt{3}V_h \sin[h\omega_1 t - \delta] \\ v_q = \sqrt{3}V_1 \cos\delta + \sqrt{3}V_h \cos[h\omega_1 t - \delta] \end{cases} \quad h = (h_v - 1) \tag{4a}$$

$$\begin{cases} v_d = \sqrt{3}V_1 \sin\delta + \sqrt{3}V_h \sin[h\omega_1 t + \delta] \\ v_q = \sqrt{3}V_1 \cos\delta + \sqrt{3}V_h \cos[h\omega_1 t + \delta] \end{cases} \quad h = (h_v + 1) \tag{4b}$$

where V_1 is the rms fundamental voltage, h is the harmonic order in dq-frame and δ is the load angle conventionally defined as:

$$\delta = \frac{\pi}{2} - \omega_1 t + \theta \tag{5}$$

As an example, from now on we will consider a negative sequence harmonic only, although the same procedure and conclusions can easily be proved to be valid for positive sequence harmonic as well. It can be considered as a "small disturbance" acting on the system, which is in a steady-state condition. Thus, the small variations method can be applied to the variables in (4):

$$\begin{cases} v_{d0} + \Delta v_d = \sqrt{3}V_1 \sin(\delta_0 + \Delta\delta) + \\ \qquad \sqrt{3}V_h \sin[h\omega_1 t + \delta_0 + \Delta\delta] \\ v_{q0} + \Delta v_q = \sqrt{3}V_1 \cos(\delta_0 + \Delta\delta) + \\ \qquad \sqrt{3}V_h \cos[h\omega_1 t + \delta_0 + \Delta\delta] \end{cases} \tag{6}$$

After some trigonometric simplifications and Taylor series expansion, the dq-voltage variation is obtained from (6) as:

$$\begin{cases} \Delta v_d = v_{dh} + (v_{q0} + v_{qh})\Delta\delta \\ \Delta v_q = v_{qh} - (v_{d0} + v_{dh})\Delta\delta \end{cases} \tag{7}$$

where the voltage harmonics of interest are:

$$\begin{cases} v_{dh} = \sqrt{3}V_h \sin[h\omega_1 t + \delta_0] \\ v_{qh} = \sqrt{3}V_h \cos[h\omega_1 t + \delta_0] \end{cases} \tag{8a}$$

$$\text{and} \begin{cases} v_{d0} = \sqrt{3}V_h \sin(\delta_0) \\ v_{q0} = \sqrt{3}V_h \cos(\delta_0) \end{cases} \tag{8b}$$

On the other hand, applying the small variations method to (2) leads to:

$$\begin{cases} v_{d0} + \Delta v_d = R(i_{d0} + \Delta i_d) + p(\Psi_{d0} + \Delta\Psi_d) - \\ \qquad (\dot{\theta}_0 + \Delta\dot{\theta})(\Psi_{q0} + \Delta\Psi_q) \\ v_{q0} + \Delta v_q = R(i_{q0} + \Delta i_q) + p(\Psi_{q0} + \Delta\Psi_q) + \\ \qquad (\dot{\theta}_0 + \Delta\dot{\theta})(\Psi_{d0} + \Delta\Psi_d) \end{cases} \tag{9}$$

In normal operation, it is assumed $i_{d0} = 0$ due to a maximum torque-per-ampere algorithm. Considering that the products $\Delta x \cdot \Delta y$ are sufficiently small, $\Delta i_{dq} = \Delta\psi_{dq}/L$, and substituting (7) in (9), the perturbations v_{dh} and v_{qh} are:

$$\begin{cases} v_{dh} = \left(\frac{R}{L} + p\right)\Delta\Psi_d - \dot{\theta}_0\Delta\Psi_q - \Psi_{q0}\Delta\dot{\theta} - \left(v_{q0} + v_{qh}\right)\Delta\delta \\ v_{qh} = \dot{\theta}_0\Delta\Psi_d + \left(\frac{R}{L} + p\right)\Delta\Psi_q + \Psi_{d0}\Delta\dot{\theta} + (v_{d0} + v_{dh})\Delta\delta \end{cases} \tag{10}$$

The model of interest in (10) is non-autonomous, due to the time varying periodic voltages v_{dh} and v_{qh} that multiply the angle variation $\Delta\delta$. Therefore, (10) cannot be solved in the time domain applying any of the simple and on-hand methods, nor in the Laplace domain. On the other hand, the amplitudes of the harmonic voltages are usually much lower than the steady-state values, therefore in the coefficient of $\Delta\delta$ we can neglect the terms v_{dh} and v_{qh}, compared to v_{d0} and v_{q0} respectively. In fact, by simulating the complete model, it will be shown that this simplification leads to acceptable results. Thus, instead of (10), we have:

$$\begin{cases} v_{dh} = \left(\frac{R}{L} + p\right)\Delta\Psi_d - \dot{\theta}_0\Delta\Psi_q - \Psi_{q0}\Delta\dot{\theta} - v_{q0}\Delta\delta \\ v_{qh} = \dot{\theta}_0\Delta\Psi_d + \left(\frac{R}{L} + p\right)\Delta\Psi_q + \Psi_{d0}\Delta\dot{\theta} + v_{d0}\Delta\delta \end{cases} \tag{11}$$

The system described by (11) is time invariant, and therefore treatable within the classic framework of transfer functions.

Additionally, the load angle derivative can be found from (5) and its variation becomes:

$$-\Delta\dot{\theta} + p\Delta\delta = 0 \tag{12}$$

B. Mechanical Aspects of the System

A basic 2DOF mechanical system consisting of a motor and its load can be described by the differential equations:

$$\begin{cases} J_m p^2\theta_m = T_{em} - K(\theta_m - \theta_L) - B\left(\dot{\theta}_m - \dot{\theta}_L\right) \\ J_L p^2\theta_L = K(\theta_m - \theta_L) - B\left(\dot{\theta}_m - \dot{\theta}_L\right) - T_L \end{cases} \tag{13}$$

where T_{em} and T_L are electromagnetic and load torque, J_m and J_L are motor and load moments of inertia, K and B are coupling stiffness and damping, θ_m and θ_L are motor and load angular mechanical positions.

Machine coupling is typically realised by two joints and a torquemeter. A simplified representation of the mechanical components, as well as the procedure for calculating the parameters K and B is shown in Appendix I.

The shaft torque T_{sh} acting on the coupling depends on the physical properties of the materials, the geometry and on the position and the speed difference of the two shafts. Thus, the shaft torque is:

$$T_{sh} = K(\theta_m - \theta_L) + B\left(\dot{\theta}_m - \dot{\theta}_L\right) \tag{14}$$

This parameter is important, above all, close to resonance condition because it is linked to the strain of the coupling and the shafts.

From (13), the transfer function relating the electromagnetic torque T_{em} and the motor electrical speed θ, can be written as:

$$\frac{\dot{\theta}}{T_{em}} = \frac{n_p(J_L p^2 + Bp + K)}{J_m J_L p^3 + B(J_m + J_L)p^2 + (J_m + J_L)Kp} = \frac{n_p N(p)}{D(p)} \tag{15}$$

where n_p is the number of pole pairs. Since we are interested in the effect of T_{em} harmonics on the speed, the load torque T_L can be considered constant, and thus it can be neglected in the derivation of (15) and in the further analysis of small variations.

After applying the small variations method to (15), the following expression is obtained:

$$T_{em0} + \Delta T_{em} = \frac{D(p)}{n_p N(p)}\left(\dot{\theta}_0 + \Delta\dot{\theta}\right) \tag{16}$$

On the other hand, the electromagnetic torque depends on the current i_q:

$$T_{em} = n_p\Psi_{PM} i_q \tag{17}$$

By (1) and by resorting to small variations, (17) becomes:

$$T_{em0} + \Delta T_{em} = \frac{n_p\Psi_{PM}}{L}\left(\Psi_{q0} + \Delta\Psi_q\right) \tag{18}$$

Equating the torque variation from (16) and (18), a relationship between the electrical and the mechanical quantities can be obtained:

$$\frac{\Psi_{PM}}{L}\Delta\psi_q - \frac{D(p)}{n_p^2 N(p)}\Delta\dot{\theta} = 0 \tag{19}$$

Finally, the overall system model consists of (11), (12) and (19). In matrix form in the Laplace domain, it is:

$$\begin{bmatrix} \frac{R}{L} + s & -\dot{\theta}_0 & -\Psi_{q0} & -v_{d0} \\ \dot{\theta}_0 & \frac{R}{L} + s & \Psi_{d0} & v_{q0} \\ 0 & \frac{\Psi_{PM}}{L} & -\frac{D(s)}{n_p^2 N(s)} & 0 \\ 0 & 0 & 1 & -s \end{bmatrix} \begin{bmatrix} \Delta\psi_d \\ \Delta\psi_q \\ \Delta\dot{\theta} \\ \Delta\delta \end{bmatrix} = \begin{bmatrix} V_{dh} \\ V_{qh} \\ 0 \\ 0 \end{bmatrix} \tag{20}$$

Once the system is solved, the flux variation $\Delta\Psi_q$ is particularly important because it gives rise to a current, and consequently, a torque variation ΔT_{em}.

$$\Delta T_{em}(s) = \frac{n_p\Psi_{PM}}{L}\Delta\psi_q(s) = G_{em,d}(s)V_{dh}(s) + G_{em,q}(s)V_{qh}(s) \tag{21}$$

The full expressions of the transfer functions $G_{em,d}$ and $G_{em,q}$ are given in (22).

$$\begin{aligned} G_{em,d}^{num}(s) &= -n_p\Psi_{PM}L\dot{\theta}_0 J_m J_L s^2\left[s^2 + Bs/J_{eq} + \omega_{N,mech}^2\right] \\ G_{em,q}^{num}(s) &= n_p\Psi_{PM}s^2(R + sL)J_m J_L\left[s^2 + Bs/J_{eq} + \omega_{N,mech}^2\right] \\ G_{em,dq}^{den}(s) &= \\ & J_m J_L s^2\left[(R + sL)^2 + \left(L\dot{\theta}_0\right)^2\right]\left[s^2 + \frac{B}{J_{eq}}s + \omega_{N,mech}^2\right] + \\ & + J_L\left(n_p\Psi_{PM}\right)^2\left[Rs + L\left(s^2 + \dot{\theta}_0^2\right)\right]\left[s^2 + \frac{B}{J_L}s + \frac{K}{J_L}\right] \end{aligned} \tag{22}$$

where $\omega_{N,mech}$ is the mechanical natural frequency and J_{eq} is the equivalent inertia, which are given by:

$$\omega_{N,mech} = \sqrt{K/J_{eq}} \tag{23}$$

$$J_{eq} = J_m J_L / (J_m + J_L) \tag{24}$$

The electromagnetic torque harmonic ΔT_{em} excites a shaft torque harmonic ΔT_{sh}. The relationship between them is given by the transfer function in (25), obtained by combining (13) (neglecting T_L), (14) and (15). The full procedure is given in Appendix II.

$$\frac{\Delta T_{sh}(s)}{\Delta T_{em}(s)} = G_{sh}(s) = \frac{J_L B s^2 + J_L K s}{J_m J_L s^3 + B(J_m + J_L)s^2 + (J_m + J_L)Ks} \tag{25}$$

By substituting (21) in (25), the shaft torque harmonic in the Laplace domain can be found:

$$\Delta T_{sh}(s) = G_{sh,d}(s) V_{dh}(s) + G_{sh,q}(s) V_{qh}(s) \tag{26}$$

where $G_{sh,d} = G_{em,d} \cdot G_{sh}$ and $G_{sh,q} = G_{em,q} \cdot G_{sh}$.

The transfer functions relating v_{dh} and v_{qh} as inputs and $\Delta T_{em,h}$ and $\Delta T_{sh,h}$ as outputs, for a system whose data are given in Appendix III, are plotted in Fig. 3. As an example, the fundamental frequency is set f_1=5Hz, T_{em0}=0.2p.u. and the system is supplied by a fundamental and a single voltage harmonic whose frequency is treated as a continuous variable.

A few not-so-trivial conclusions can be drawn:

- As the electromagnetic torque frequency f_h approaches the mechanical natural frequency $f_{N,mech}=\omega_{Nmech}/(2\pi)$, the amplitude of this torque harmonic $T_{em,h}$ tends to zero. In fact, since the motor angle variation becomes significant at $f_{N,mech}$, it affects severely the back-emf variation, therefore the current harmonic spectrum changes causing the relevant $T_{em,h}$ to vanish. From a mathematical point of view, the pole in the transfer function (15) becomes a zero in (22). Therefore, the initially critical point for the system $f_{N,mech}$ does not exist anymore. Methods for damping $T_{em,h}$ cannot be applied here because this point of operation is not a threat to the system anymore.
- At the same time, the corresponding shaft torque harmonic $T_{sh,h}$ starts increasing.
- At a slightly higher frequency $f_h=f_N$, both $T_{em,h}$ and $T_{sh,h}$ reach a peak value. The new resonance frequency for the voltage-driven system is identified, whose value can be found by solving numerically the equation $G_{em,dq}^{den}(s) = 0$. At this point, the oscillation threatening to damage the shaft becomes critical.
- Even without any mechanical damping, the peak values remain limited due to the energy dissipated by the motor resistance.

One should have in mind that in practice, only discrete points of these curves exist, since there is a limited number of harmonics related to a given fundamental frequency.

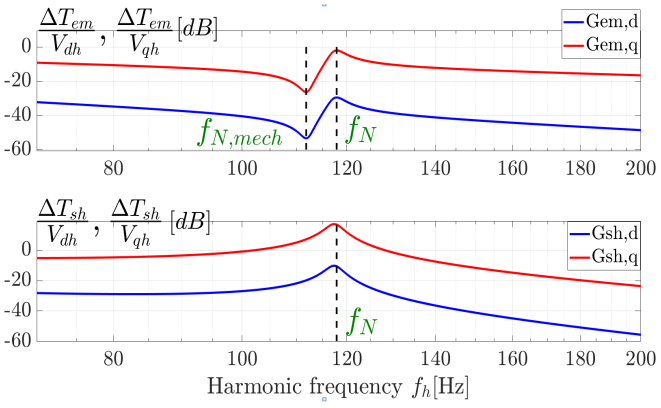

Fig. 3. Bode magnitude response to a voltage harmonic. Transfer functions from v_{dh} and v_{qh} to ΔT_{em} and ΔT_{sh}.

C. Torque Harmonics Evaluation

All the transfer functions obtained in Section II.B show relationships between the inputs v_{dh}, v_{qh} and the outputs $T_{em,h}$ and $T_{sh,h}$. However, a harmonic phase voltage v_h at frequency $\omega_h=h\cdot\omega_1$ generates simultaneously both perturbations in v_d and v_q. Thus, the torque response must combine these two contributions in a unique formula.

Equations (21) and (26) in the time domain have the same representation:

$$T_h(t) = \sqrt{3} V_h [k_1 \sin(\omega_h t + \delta_0) + k_2 \cos(\omega_h t + \delta_0)] \tag{27}$$

where the gains k_1 and k_2 depend on the magnitude and the phase of the transfer functions G_d and G_q evaluated at the forcing frequency ω_h:

$$k_1 = |G_d(j\omega_h)| \cos\left(arg(G_d(j\omega_h))\right) - |G_q(j\omega_h)| \sin\left(arg\left(G_q(j\omega_h)\right)\right) \tag{28.1}$$

$$k_2 = |G_d(j\omega_h)| \sin\left(arg(G_d(j\omega_h))\right) + |G_q(j\omega_h)| \cos\left(arg\left(G_q(j\omega_h)\right)\right) \tag{28.2}$$

where the transfer functions $G_d \in \{G_{em,d}, G_{sh,d}\}$ and $G_q \in \{G_{em,q}, G_{sh,q}\}$ respectively.

Finally, the torque harmonic amplitude is computed as:

$$|T_h| = \sqrt{3} V_h \sqrt{k_1^2 + k_2^2} \tag{29}$$

When it is not measured, an approximate value of V_h in practical conditions can be found by using the well-known formula, valid for sinusoidal PWM modulation:

$$V_h = \frac{\sqrt{2} V_{dc}}{m \cdot \pi} J_n\left(m \frac{m_a \pi}{2}\right) \sin\left([m+n]\frac{\pi}{2}\right) \tag{30}$$

where V_{dc} is the dc voltage supply, m_a is the amplitude modulation index, m and n are indices related to the voltage harmonic order $h_v=m\cdot m_f+n$, m_f is the frequency modulation index and $J_n(\cdot)$ is the Bessel function of first type of order n. The harmonic components which typically exist in the three-phase output voltage of an inverter with SPWM are of order $h_v \in \{1, m_f \pm 2, 2m_f \pm 1, 3m_f \pm 2, 4m_f \pm 1, \ldots\}$.

As an example, let us analyse the $h=m_f+3$ torque harmonic resulting from an $h_v=m_f+2$ phase voltage harmonic, with m_f=15. At varying fundamental frequency and a fixed harmonic order, the torque amplitudes calculated by (29) are

plotted in Fig. 4. In this plot, each point represents operation at steady state.

Conclusions like those at point B can be drawn:

- When $f_h = f_{N,mech}$, $T_{em,h} \approx 0$ and $T_{sh,h}$ increases.
- At $f_h = f_{N,mech}$, both $T_{em,h}$ and $T_{sh,h}$ reach a peak value.
- The peak values of the torque harmonic amplitudes are limited.

In case of more phase voltage harmonics contributing to the same torque harmonic, superposition of the effects can be applied. The procedure explained in Sec. II should be repeated for each v_h separately, and the resulting torque components at the same frequency are superposed in the time or the frequency domain.

III. Simulation Results

Initially, the individual transfer functions $G_{em,d}$, $G_{em,q}$, $G_{sh,d}$ and $G_{sh,q}$ were verified in Matlab/Simulink environment. Model parameters are given in Appendix III. The PMSM was supplied by a fundamental phase voltage and a sinusoidal perturbation in the voltages v_d and v_q, respectively. The results are given in Fig. 5a for several different harmonic frequencies, where the points represent simulation results, and the dashed lines are obtained analytically. The fundamental frequency was f_1=5Hz and the electromagnetic torque T_{em0}=0.2p.u. Another example is shown in Fig. 5b, where f_1=9.33Hz and T_{em0}=0.36p.u.

The errors in predicting both the electromagnetic and the shaft torque harmonics are about 1%, as evident from Fig. 5. It means the approach of neglecting the terms v_{dh} and v_{qh} in the coefficient of $\Delta\delta$ is justified.

The next step was to verify the formula in (29) proposed for predicting analytically the amplitudes of the harmonics $T_{em,h}$ and $T_{sh,h}$. Considering again a torque harmonic h=m_f+3=18, the fundamental frequency was varied in such a way that the harmonic frequency f_h=$h f_1$ fell within an interval containing the natural frequency f_N. The results are shown in Fig. 6, where each point represents a steady-state point of operation. It can be seen that calculated values match almost perfectly the simulation results.

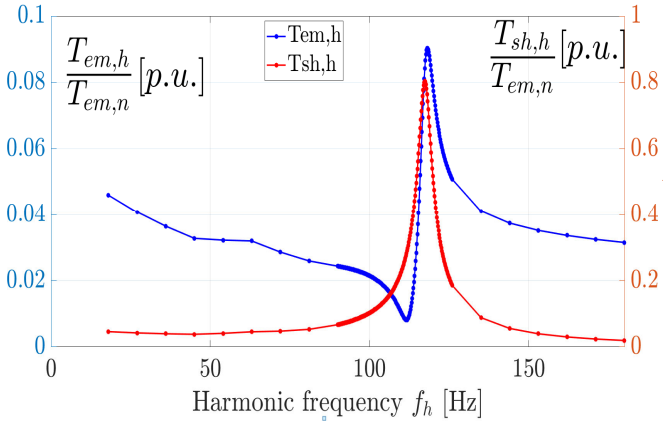

Fig. 4. Amplitudes of the h=m_f+3=18th electromagnetic $T_{em,h}$ and shaft $T_{sh,h}$ torque harmonic when the system is supplied by h_v=m_f+2=17th phase voltage harmonic. Each point represents operation at steady state. At $f_{N,mech}$ there is almost zero $T_{em,h}$. At f_N, both $T_{em,h}$ and $T_{sh,h}$ reach peak value.

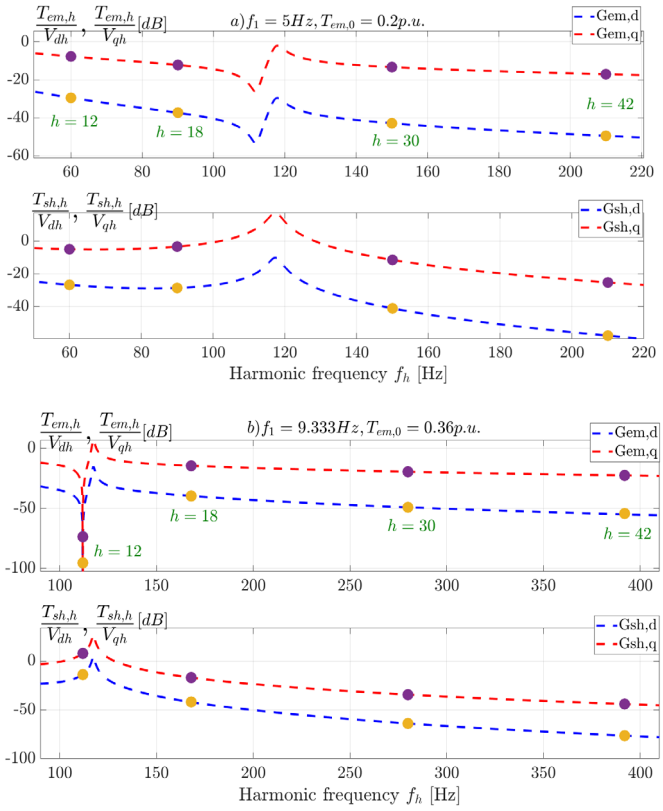

Fig. 5. Transfer functions between the inputs v_{dh} and v_{qh} and the outputs $T_{em,h}$ and $T_{sh,h}$ for fixed f_1 and variable harmonic frequency. Comparison between analytical (dashed line) and simulated results (points) for two different cases: a) f_1 = 5Hz, T_{em0}=0.2p.u. b) f_1 = 9.33Hz, T_{em0}=0.36p.u.

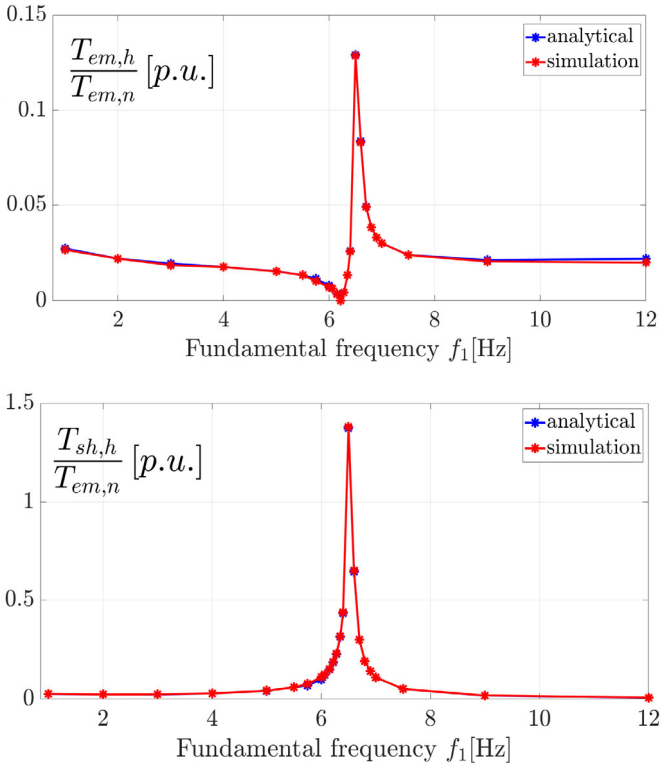

Fig. 6. Amplitude of the h=m_f+3=18th electromagnetic and shaft torque harmonic for various fundamental frequencies.

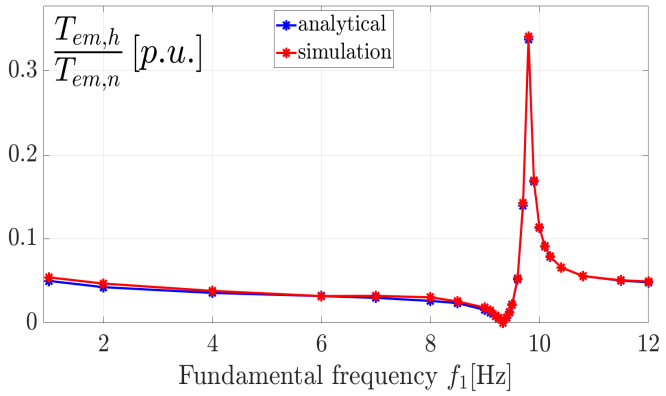

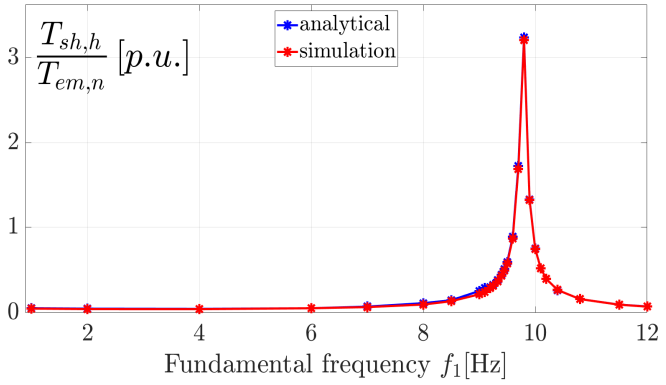

Fig. 7. Amplitude of the h=m_f–3=12th electromagnetic and shaft torque harmonic for various fundamental frequencies.

IV. Conclusions

In this paper, a mathematical model of a PMSM operating in/around resonance was presented, accounting for the harmonic voltage supply, coupling characteristics and load equation. Simple formulae were obtained for predicting the electromagnetic- and shaft-torque harmonic amplitudes caused by a supply harmonic voltage. The model was proved to provide accurate results in simulation environment. The trend of a specific torque harmonic amplitude can indicate when the system approaches resonance, which is very helpful for field engineers who should take suitable measures.

V. Appendix I

A simple representation of the PMSM, its load (in this case, a dc machine), and their coupling elements is shown in Fig. 8.

Equivalent coupling stiffness considers a series connection of all the elements, thus:

$$\frac{1}{K}=\frac{1}{K_m}+\frac{1}{K_{c1}}+\frac{1}{K_{tm}}+\frac{1}{K_{c2}}+\frac{1}{K_L} \qquad \text{(AI.1)}$$

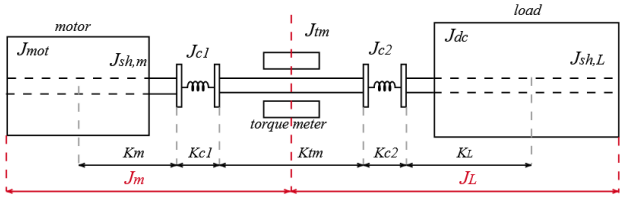

Fig. 8. System components relevant for computing the mechanical parameters. PMSM and a dc machine coupled by two joints and a torquemeter.

where the stiffness of the couplings K_{c1}, K_{c2} and the torquemeter K_{tm} can be read from the manufacturer datasheets. The stiffness of the shaft segments is calculated accounting for the material shear modulus G, external diameter $D_{m,L}$, shaft length $l_{m,L}$:

$$K_{m,L}=\frac{\pi G D_{m,L}^4}{32 l_{m,L}} \qquad \text{(AI.2)}$$

Coupling damping is typically one percent of the critical damping, which is related to the inertias as:

$$B_{cr}=2J_{eq}\omega_{N.mech} \qquad \text{(AI.3)}$$

Motor and load inertia are:

$$J_m=J_{mot}+J_{sh,m}+J_{c1}+J_{tm}/2 \qquad \text{(AI.4.1)}$$

$$J_L=J_{tm}/2+J_{c2}+J_{sh,L}+J_{dc} \qquad \text{(AI.4.2)}$$

VI. Appendix II

Equation (15) can be written in the Laplace domain:

$$\begin{cases} J_m s^2\theta_m = T_{em}-K(\theta_m-\theta_L)-B(\dot\theta_m-\dot\theta_L) \\ J_L s^2\theta_L = K(\theta_m-\theta_L)-B(\dot\theta_m-\dot\theta_L)-T_L \end{cases} \qquad \text{(AII.1)}$$

Expressing the angular positions through the speeds as $\theta_{m,L}=\dot\theta_{m,L}/s$ leads to:

$$\begin{cases} J_m s\dot\theta_m = T_{em}-(B+K/s)(\dot\theta_m-\dot\theta_L)=T_{em}-T_{sh} \\ J_L s\dot\theta_L = (B+K/s)(\dot\theta_m-\dot\theta_L)-T_L=T_{sh}-T_L \end{cases} \qquad \text{(AII.2)}$$

Equation (AII.2) can be represented by the block scheme in Fig. 9. After a few simplification steps, the open-loop transfer function L_{sh}(s) between the electromagnetic torque T_{em} and the shaft torque T_{sh} (Fig. 10) is given in (AII.4), and the closed-loop transfer function G_{sh}(s) in (AII.5).

$$\frac{T_{sh}(s)}{\dot\theta_m(s)}=\frac{J_L B s^2+J_L K s}{J_L s^2+B s+K} \qquad \text{(AII.3)}$$

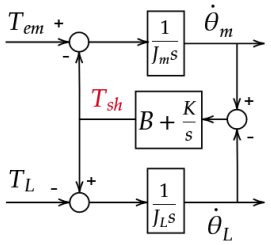

Fig. 9. Block-scheme representation of (AII.2) in the Laplace domain.

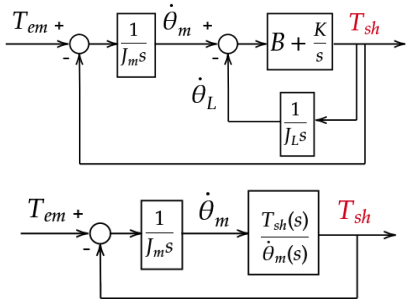

Fig. 10. Simplification steps of the block-scheme in Fig. 9

$$L_{sh}(s) = \frac{1}{J_m s} \cdot \frac{T_{sh}(s)}{\dot{\theta}_m(s)} \quad \text{(AII.4)}$$

$$\frac{T_{sh}(s)}{T_{em}(s)} = \frac{L_{sh}(s)}{1+L_{sh}(s)} = G_{sh}(s) \quad \text{(AII.5)}$$

VII. APPENDIX III

TABLE I
PMSM, LOAD AND COUPLING DATA

Rated power P_n [kW]	6.91
Rated torque $T_{em,n}$ [Nm]	22
Number of pole pairs n_p	3
Rated frequency f_n [Hz]	150
Permanent magnet flux Ψ_{PM} [Wb]	0.165
Phase resistance R [Ω]	0.393
Synchronous inductance L_d=L_q=L [H]	$4.8 \cdot 10^{-3}$
Motor side inertia J_m [kg·m^2]	$3 \cdot 10^{-3}$
Load side inertia J_L [kg·m^2]	$123 \cdot 10^{-3}$
Coupling stiffness K [Nm/rad]	1458.5
Coupling damping B [Nms/rad]	0.0567

VIII. REFERENCES

[1] M. Bruha, "Electro-mechanical interaction between electric drive and its mechanical load and control interventions mitigating unwanted vibration phenomena," Ph.D. dissertation, Faculty of Electr. Engin., Univ. of West Bohemia, Pilsen, Czech Republic, 2018.

[2] J. Song-Manguelle, G. Ekemb, D. L. Mon-Nzongo, T. Jin and M. L. Doumbia, "A theoretical analysis of pulsating torque components in ac machines with variable frequency drives and dynamic mechanical loads," *IEEE Trans. on Industrial Electronics*, vol. 65, no. 12, pp. 9311-9324, Dec. 2018.

[3] D. L. Mon-Nzongo, G. Ekemb, J. Song-Manguelle, P. G. Ipoum-Ngome, T. Jin and M. L. Doumbia, "LCIs and PWM-VSIs for the Petroleum industry: a torque oriented evaluation for torsional analysis purposes," *IEEE Trans. on Power Electronics*, vol. 34, no. 9, pp. 8956-8969, Sept. 2019.

[4] J. S. Manguelle, C. Sihler and J. M. Nyobe-Yome, "Modeling of torsional resonances for multi-megawatt drives design," *2008 IEEE Industry Society Annual Meeting*, pp. 1-8, Nov. 2008.

[5] Y. Liao, L. Ran, G. A. Putrus and K. S. Smith, "Evaluation of the effects of rotor harmonics in a doubly-fed induction generator with harmonic induced speed ripple," *IEEE Trans. on Energy Conversion*, vol. 18, no. 4, pp. 508-515, Dec. 2003.

[6] E. G. Hauptmann, W. F. Eckert and B. C. Howes, "The influence on torsional vibration analysis of electromagnetic effects across an induction motor air gap," presented at the Gas Machinery Conference, Albuquerque, New Mexico, USA, 6 Oct. 2013, pp. 1-11.

[7] T. Feese and A. Kokot, "Electromagnetic effects on the torsional natural frequencies of an induction motor driven reciprocating compressor with a soft coupling," 45th Turbomachinery and 32nd Oump Symposia, Huston, Texas, 12-15 Sept. 2016, pp. 1-22.

[8] J. Licari, C. E. Ugalde-Loo, J. Liang, J. Ekanayake and N. Jenkins, "Torsional damping considering both shaft and blade flexibilities," *Wind Engineering*, vol. 36, no. 2, pp. 181-195, 2012.

IX. BIOGRAPHIES

Dejan Pejovski received his MS degree in electrical engineering at Politecnico di Milano, Milano, Italy in 2019. Currently, he is a PhD student in Electrical Engineering at Politecnico di Milano. His interests are in power electronics, electrical machines and drives.

Antonino Di Gerlando received his MS degree in electrical engineering from the Politecnico di Milano, Italy, in 1981. Currently, he is a Full Professor at the Department of Energy at Politecnico di Milano. Fields of interest: design and modelling of electrical machines, converters and drive systems. He is a senior member of IEEE, and member of the Italian Association AEIT.

Giovanni Maria Foglia received his MS degree and the PhD in electrical engineering from the Politecnico di Milano, Milano, Italy, in 1997 and 2000. Currently, he is an Assistant Professor at the Department of Energy at Politecnico di Milano, and his main field of interest is the analysis and design of PM electrical machines.

Roberto Perini (M'10) received his MS degree and the PhD in electrical engineering from the Politecnico di Milano, Milano, Italy. Currently, he is an Associate Professor at the Department of Energy at Politecnico di Milano. His interests are in the design and modelling of electrical machines and power electronics.